International Journal of Signal and Imaging Systems Engineering

ISSN online: 1748-0701 - ISSN print: 1748-0698
https://www.inderscience.com/ijsise

Intelligent fault diagnosis of multi-sensor rolling bearings based on variational mode extraction and a lightweight deep neural network

Shouqi Wang, Zhigang Feng

DOI: 10.1504/IJSISE.2024.10061695

Article History:

Received:	09 April 2023
Last revised:	14 December 2023
Accepted:	18 December 2023
Published online:	15 July 2024

Intelligent fault diagnosis of multi-sensor rolling bearings based on variational mode extraction and a lightweight deep neural network

Shouqi Wang and Zhigang Feng*

Department of Automation,
Shenyang Aerospace University,
Shenyang, 110136, China
Email: wsq1120bf@163.com
Email: fzg1023@yeah.net
*Corresponding author

Abstract: After a rolling bearing failure in an industrial complex environment, the vibration signals collected by the sensors can easily be corrupted by a wide range of noise information, affecting the effectiveness of the feature extraction process. Although deep learning models can extract fault features better, most of the models currently used have complex structures with many parameters and cannot be deployed in embedded environments. In this paper, we propose an intelligent fault diagnosis method combining variational mode extraction (VME) with lightweight deep neural networks, which has the advantages of anti-noise robustness and model lightweight. Firstly, VME is used to process the vibration signals of different sensors to obtain the required modal component signals and convert them into greyscale images. Subsequently, the improved lightweight deep neural network Bypass-SqueezeNet is used for fault diagnosis. Several experiments are conducted on the experimental dataset, and the final experimental results prove that the method proposed in this paper possesses more satisfactory diagnostic performance.

Keywords: rolling bearing; intelligent fault diagnosis; VME; variational mode extraction; lightweight deep neural network.

Reference to this paper should be made as follows: Wang, S. and Feng, Z. (2024) 'Intelligent fault diagnosis of multi-sensor rolling bearings based on variational mode extraction and a lightweight deep neural network', *Int. J. Signal and Imaging Systems Engineering*, Vol. 13, No. 1, pp.27–40.

Biographical notes: Shouqi Wang received his Bachelor's degree in Measurement and Control Technology and Instruments from Shenyang Aerospace University in 2021, and he is currently studying for a Master's degree at Shenyang Aerospace University. His research direction is intelligent fault diagnosis, deep learning, machine learning.

Zhigang Feng received his MS and the PhD in Measurement and Control Technology and Instrumentation from Harbin Institute of Technology in 2005 and 2009 respectively. In April 2009, he came to Shenyang Aerospace University to teach. He has been engaged in the research of sensor information processing, selfvalidating sensor, self-validating actuator and automatic test system, and has a solid theoretical foundation and practical experience. He has participated in the research and development of many aviation and aerospace projects, and published more than 30 papers.

1 Introduction

With the development of computer and sensor technology, the condition monitoring of mechanical equipment has entered the 'big data' era. Rolling bearings, as the core components of mechanical equipment in many fields such as transportation, aerospace, and electric power, work in a high-temperature, heavy-duty environment for a long period of time and are highly susceptible to failures that can lead to catastrophic accidents (Zhen et al., 2022). Rolling bearing fault diagnosis also needs to realise automation, intelligence, and systematisation, thus avoiding safety accidents and major economic losses, so how to make from the mechanical equipment 'big data' in the mining representative information has become the focus of the current researchers to explore the direction.

The fault diagnosis mode of rolling bearings has experienced three stages: manual fault feature extraction, machine learning diagnosis, and deep learning diagnosis. Early manual extraction of fault features is mainly recognised by eliminating the noise signals in the original signal to extract fault features through signal processing methods such as variational mode decomposition (VMD) (Sheoran and Saini, 2021), wavelet transform (WT) (Mourad et al., 2010), discrete cosine transform (DCT) (Walia et al., 2015), intrinsic time scale decomposition (ITD) (Yu and Pan, 2020), and so on. Xu et al. (2021a) experimentally discovered the similarity of sub-signals in singular value decomposition (SVD) and used SVD in conjunction with squared envelope spectroscopy (SES) to extract weak fault signals. Li et al. (2022b) used a parameter optimisation approach to determine the VMD parameters, which ultimately enabled the diagnosis of composite bearing faults in different frequency bands. Yu and Pan (2020) proposed an ITD-GSP approach that can extract composite faults in rolling bearings to achieve diagnosis. While the methods described above are capable of effective fault diagnosis, the use of manual extraction of fault features relies on expert empirical knowledge, and features that are applicable to one device may not be valid on another.

The development of sensor technology makes the collection of signals more convenient, and a large number of data-driven intelligent algorithms are widely used in the field of fault diagnosis, among which the machine learning algorithms represented by support vector machines (SVM) (Kim, 2014) and artificial neural networks (ANN) (Zhang and Gao, 2013) have good diagnostic effects, which have greatly contributed to the innovation of the diagnostic modes of mechanical equipment. However, these algorithms require time to manually extract useful features and still require expert experience. In the meantime, machine learning algorithms are prone to overfitting problems when dealing with large-scale data, resulting in a low final accuracy rate. When processing data containing noise, machine learning algorithms can only extract the surface features of a vibration signal, so their learning ability is limited and they cannot achieve satisfactory recognition accuracy.

Deep learning-based fault diagnosis methods are able to obtain representative fault information from input data, realise automatic extraction of features, approximate complex nonlinear functions with small errors, have excellent feature processing capabilities, and have received very much attention in rotating machinery fault diagnosis research (Azim Naz and Sarath, 2022). However, there are two problems that need to be solved in the above fault diagnosis methods. The first problem is that rolling bearings mostly work in complex environments, which are often accompanied by the influence of noise. Noise has a significant impact on the model learning process, which can drastically reduce the final diagnosis accuracy (Liang et al., 2022). Another problem is that most of the current models occupy a huge amount of memory, and as the model complexity increases, the number of parameters in the model is also increasing dramatically, which cannot meet the requirements of simplicity and efficiency in industrial applications (Zhong et al., 2022). Based on the above issues, some scholars have already been conducting research. Feng et al. (2023) designed a multilevel noise reduction model based on intrinsic time scale decomposition and improved SVD, which, combined with an improved convolutional neural network (CNN), can realise highly accurate fault diagnosis of rolling bearings in a strongly noisy industrial environment. Liang et al. (2022) constructed a network model named WT-IResNet, which possesses high diagnostic accuracy with good results in noisy backgrounds. Wang and Feng (2024) design a multi-band greyscale feature map fusing information from multiple sensors, combined with a lightweight UL-GoogLeNet model for diagnosis, which not only achieves high-performance diagnosis under noise interference but also realises the lightweight application of the model.

In this paper, in order to solve the problems of the poor diagnostic effect of rolling bearings in the noise interference environment and the complexity of the model with huge parameters, a method of intelligent fault diagnosis of multi-sensor rolling bearings based on VME and a lightweight deep neural network is designed. The bearing vibration signals collected from multiple sensors are first processed to obtain the desired modal component signals using variational mode extraction (VME), which removes the effect of noise from the signals. The one-dimensional modal component signals are then converted into a 2D greyscale image, and a new greyscale image is obtained by stitching. Subsequently, a lightweight Bypass-SqueezeNet model is built, and the model is trained and tested using greyscale images for eventual fault diagnosis.

2 Theoretical knowledge

2.1 Variational mode extraction (VME)

VME is a method for extracting the modal components of a particular signal with very low computational complexity and will decompose the input signal $f_r(t)$ into the desired mode $u_d(t)$ and the residual signal $f_r(t)$ (Li et al., 2022a). For the desired mode $u_d(t)$, which transforms its analytic signal by Hilbert and then compacts at the predicted center frequency, the variational expression is:

$$J_1 = \left\| \partial_t \left[\left(\delta(t) + \frac{j}{\pi t} \right) * u_d(t) \right] e^{-jw_d t} \right\|_2^2 \tag{1}$$

where δ is the Dirac distribution and $*$ denotes the convolution.

In the process of extracting the desired mode $u_d(t)$, the spectral overlap between the residual signal $f_r(t)$ and the desired mode $u_d(t)$ is 0, i.e., the energy of the residual signal is minimised at the frequency band where the desired mode is located. Therefore, a penalty function is introduced:

$$J_2 = \| \beta(t) * f_r(t)) \|_2^2 \tag{2}$$

where $\beta_{(t)}$ is the impulse response of the frequency response filter used.

The variational problem of finding the expected modes under the condition that $f(t) = u_d(t) + f_r(t)$ is satisfied:

$$\min_{\alpha_{d,\omega_d}, f} \{\alpha J_1 + J_2\} \\ \text{subject to: } u_d(t) + f_r(t) = f(t) \tag{3}$$

where α is the parameter used to balance J_1 and J_2.

The VME transforms the constrained variational problem into an unconstrained variational problem by using the alternating direction multiplication operator to find the saddle point of the Lagrange function, i.e., the optimal solution of equation (3), to obtain the desired modes.

2.2 *SqueezeNet model*

SqueezeNet is a simple CNN architecture that decreases the depth as well as the parameters of the network while maintaining the classification accuracy of the model (Kajkamhaeng and Chantrapornchai, 2021). Unlike networks such as ResNet and AlexNet, which deepen the network structure to improve accuracy, SqueezeNet reduces training costs while ensuring improved model accuracy. The important part of SqueezeNet is the Fire module, which is composed of the Squeeze layer and the Expand layer, and its structure is shown in Figure 1. The Squeeze layer is a convolutional layer composed of only 1×1 convolutional kernels, and the Expand layer is composed of 1×1 and 3×3 convolutional kernels. The number of convolutional kernels in the Squeeze layer and the Expand layer needs to satisfy the requirements of $s_{1\times1} < e_{1\times1} + e_{3\times3}$ (Iandola et al., 2016). As shown in Figure 2(a), the SqueezeNet model uses the Fire module instead of a large number of convolutional and pooling layers to compress the feature image dimensions and reduce the network structure, avoiding the high-intensity computation of a redundant network and reducing the hardware requirements to some extent.

Figure 1 Fire module structure

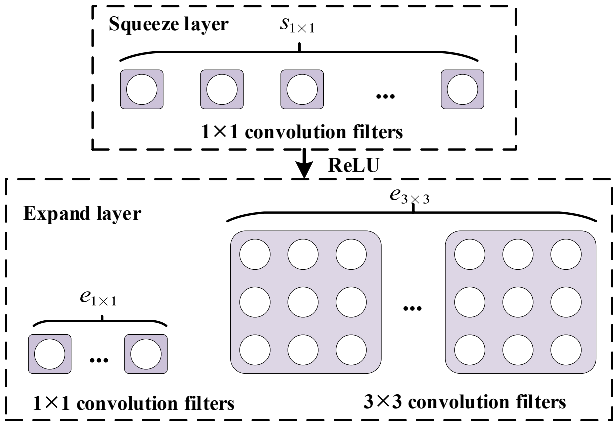

Figure 2 (a) SqueezeNet model structure and (b) bypass-SqueezeNet model structure (see online version for colours)

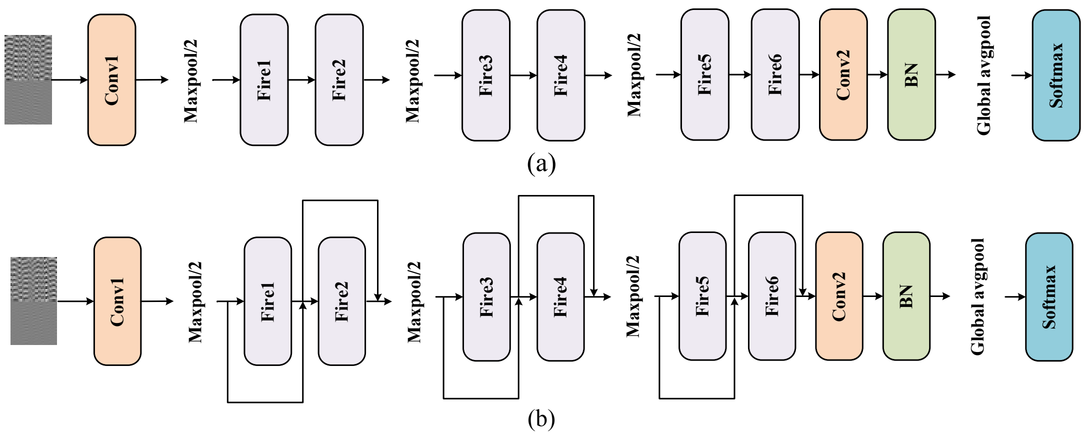

The improved Bypass-SqueezeNet model in this paper is shown in Figure 2(b). Based on SqueezeNet, this model adds residual connections beside the Fire modules, and the input features and output features from the Fire module will be used as the inputs of the next module after summing, which can realise multi-layer crossing of information and solve the problems of gradient vanishing and gradient explosion. Through the superposition of multiple Fire modules, the deep feature extraction ability of the model can be enhanced, accelerating its training speed and improving its diagnostic accuracy rate.

3 The proposed method

In order to learn the fault features of rolling bearings more effectively and improve the diagnostic performance and accuracy of the diagnostic model, this paper proposes a multi-sensor intelligent fault diagnosis method for rolling bearings based on VME and a lightweight deep neural network.

Firstly, this paper uses the rolling bearing vibration signals from multiple sensors, and the data from different sensors cooperating for fault diagnosis can learn more reliable results through a more complete dataset, avoid losing important fault features, and improve the robustness and accuracy of the diagnostic model (Shao et al., 2021; Xie et al., 2022). The vibration signals of different sensors are processed by the VME algorithm to extract the modal component signals and eliminate the influence of noise signals. Then each modal component is converted into a 2D greyscale image, and the greyscale images of different sensors are spliced into a new greyscale image. Next, the greyscale images are divided into a training set and a testing set, and the training set is input into the Bypass-SqueezeNet model for training. Finally, the testing set is input into the trained Bypass-SqueezeNet model for testing, and the results of the fault diagnosis are obtained. The framework of the proposed method is shown in Figure 3. The specific steps are as follows:

Step 1: Collect the vibration signal of the rolling bearing. Multiple acceleration sensors are installed on the experimental device, and the experiment is carried out by collecting the vibration signal of each sensor.

Step 2: Use the VME algorithm to process the vibration signals of each sensor. The VME algorithm needs to determine two key parameters: penalty factor α and initial center frequency ω_d. In this paper, the above two parameters are determined by the method proposed in Ye et al. (2023), in which the penalty factor $\alpha = 1000$ and the initial center frequency ω_d are determined by the frequency of the highest spectral peak of the bearing vibration signal.

Step 3: The modal component signals obtained by VME processing are converted into 2D greyscale images, and the detailed conversion process is shown in Figure 4. Assuming that the signal has a length of l data points, it can be converted into an N-row vector with M data points, where $l = M \times N$. The length of the vibration signal in the paper $l = 1024$ is finally converted into a 32×32 matrix. The data needs to be normalised before it is converted into a matrix, and the normalisation formula is:

$$y = \frac{x - \min}{\max - \min} \times 255 \tag{4}$$

where x and y represent the values before normalisation and normalised, respectively, and max and min represent the maximum and minimum values in the data.

Figure 3 The framework of the proposed method (see online version for colours)

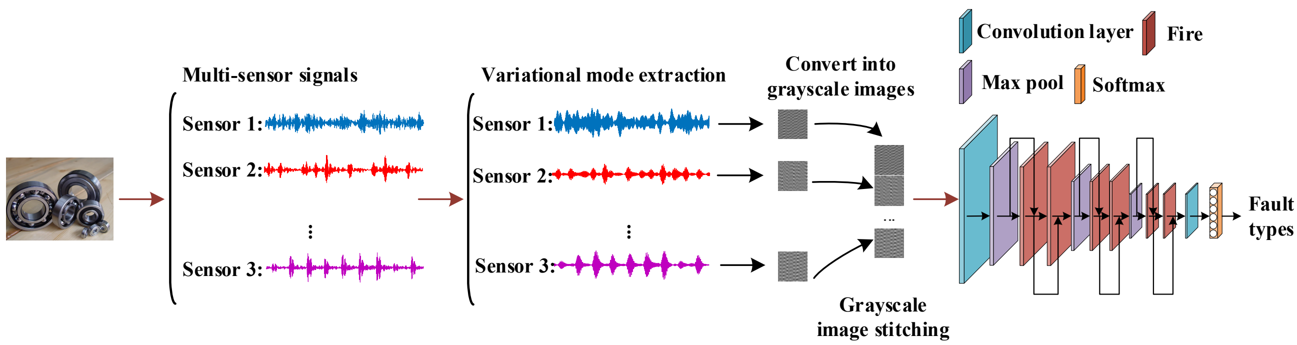

Figure 4 The process of transforming a greyscale image (see online version for colours)

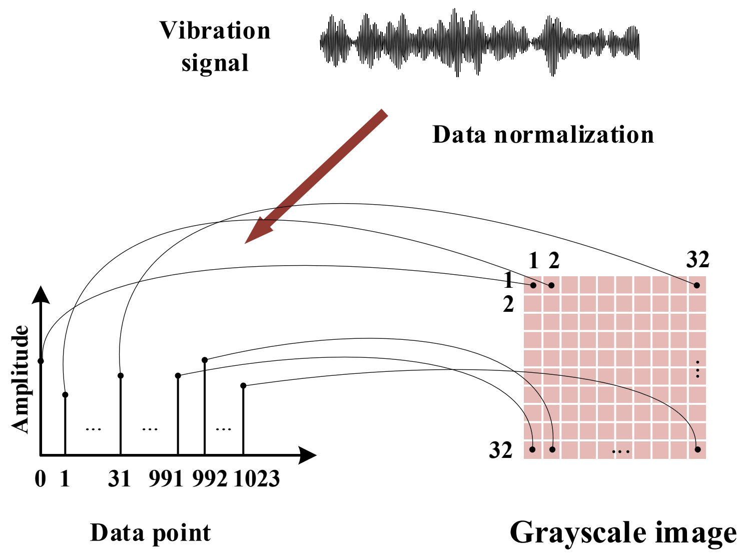

Then, the greyscale images converted from the modal components of the vibration signals of multiple sensors are spliced to facilitate the training and testing of the subsequent network model.

Step 4: Divide the dataset and randomly select 80% of the greyscale image samples as the training set and 20% as the testing set, with no overlap between the samples in the training and testing sets.

Step 5: Build the Bypass-SqueezeNet model. The training set is imported into the model to adjust the parameters and train, and the trained model is saved.

Step 6: Rolling bearing fault type identification is performed, and the final diagnostic results are obtained by diagnosing the testing set using the trained model.

4 Experimental verification and analysis

The method proposed in this paper is written on Matlab R2021b software, a computer using Windows 10 64-bit, a CPU model AMD Ryzen 5 5600U with Radeon Graphics 2.30 GHz, a GPU model NVIDIA Gefore MX450, and a Case Western Reserve University (CWRU) bearing dataset for conducting experiments.

4.1 Introduction to dataset

The physical diagram of the experimental platform of the CWRU is shown in Figure 5, which consists of a motor, a torque sensor/translator, a power test meter, and an electronic controller (Smith and Randall, 2015).In this paper, the bearing data of the drive end (DE) and fan end (FE) under the conditions of 1772 r/min rotational speed and 12 kHz sampling frequency are selected. The bearing datasets of two accelerometers (sensors) at the DE and FE are established. Using EDM to manually add faults to the rolling bearings, there are three different levels of damage: 0.007, 0.014, and 0.021 inches, respectively, and the fault data are detailed in Table 1.

Figure 5 CWRU bearing experiment platform (see online version for colours)

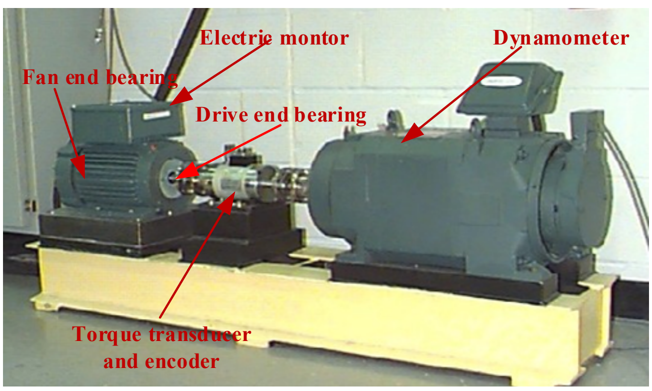

Table 1 Description of CWRU bearing fault data

Bearing status	*Accelerometer*	*Diameter* (in.)	*Class label*	*Data length*	*Sample number*
Normal	DE and FE	–	Nor	1024	200
Rolling element fault		0.007	Ba1	1024	200
		0.014	Ba2	1024	200
		0.021	Ba3	1024	200
Inner ring fault		0.007	In1	1024	200
		0.014	In2	1024	200
		0.021	In3	1024	200
Outer ring fault		0.007	Ou1	1024	200
		0.014	Ou2	1024	200
		0.021	Ou3	1024	200

As shown in Figure 6, in order to obtain more samples, this paper intercepts data with $L = 1024$ points, the overlap length between adjacent data $S = 512$. Each fault type captures 200 samples, and a total of 2000 samples for each bearing dataset.

Figure 6 Overlapping sampling method of bearing data (see online version for colours)

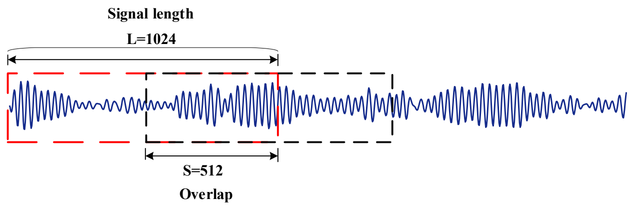

4.2 VME feature extraction experiment

The modal components of the rolling bearing vibration signals acquired by DE and FE are extracted using the VME algorithm, and Figure 7 illustrates the time-domain waveforms of the rolling bearing vibration signals acquired by DE and FE. According to the method in Section 3, the penalty factor $\alpha = 1000$ is set, and the spectrum of Ba1 vibration signals in DE and FE is given in Figure 8. From which it can be seen that the center frequencies of the highest spectral peaks are about 3400 Hz and 4100 Hz, and thus the initial center frequencies ω_d are 3400 Hz and 4100 Hz, respectively. The initial center frequencies of bearing vibration signals of different fault types are shown in Table 2.

Figures 9 and 10 shows the time-domain waveforms and spectra before and after processing the vibration signals of Ba1 at the DE and FE using VME, which can perfectly extract the modal component signals at the required center frequency. According to the method in Figure 4, the length of each signal is 1024, which is converted into a 32×32 greyscale image. Subsequently, the greyscale images of the two sensors are spliced into a 32×64 greyscale image. The greyscale images of each fault type are shown in Figure 11.

Figure 7 Time-domain waveform of bearing vibration signals for DE and FE (see online version for colours)

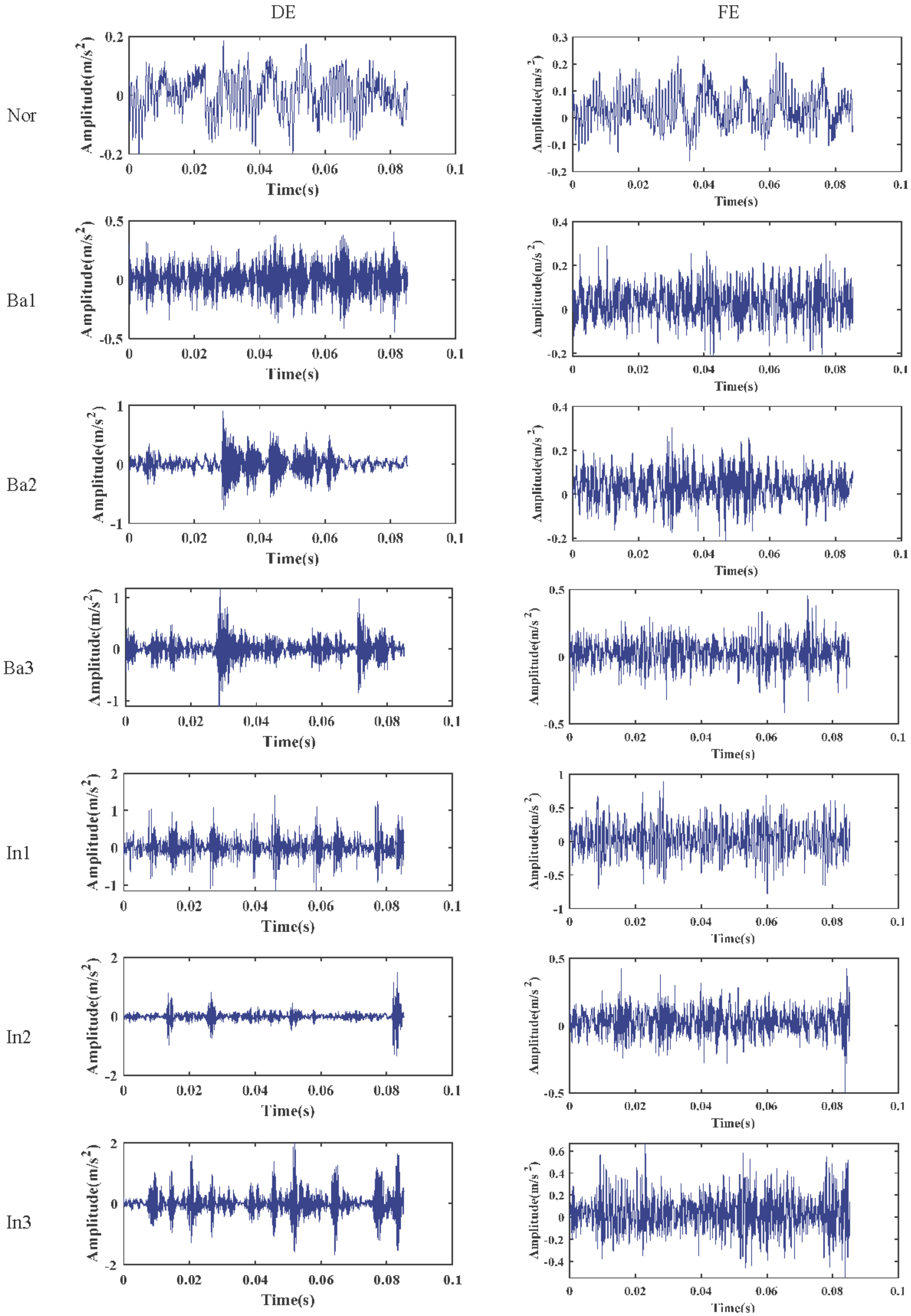

Figure 7 Time-domain waveform of bearing vibration signals for DE and FE (see online version for colours) (continued)

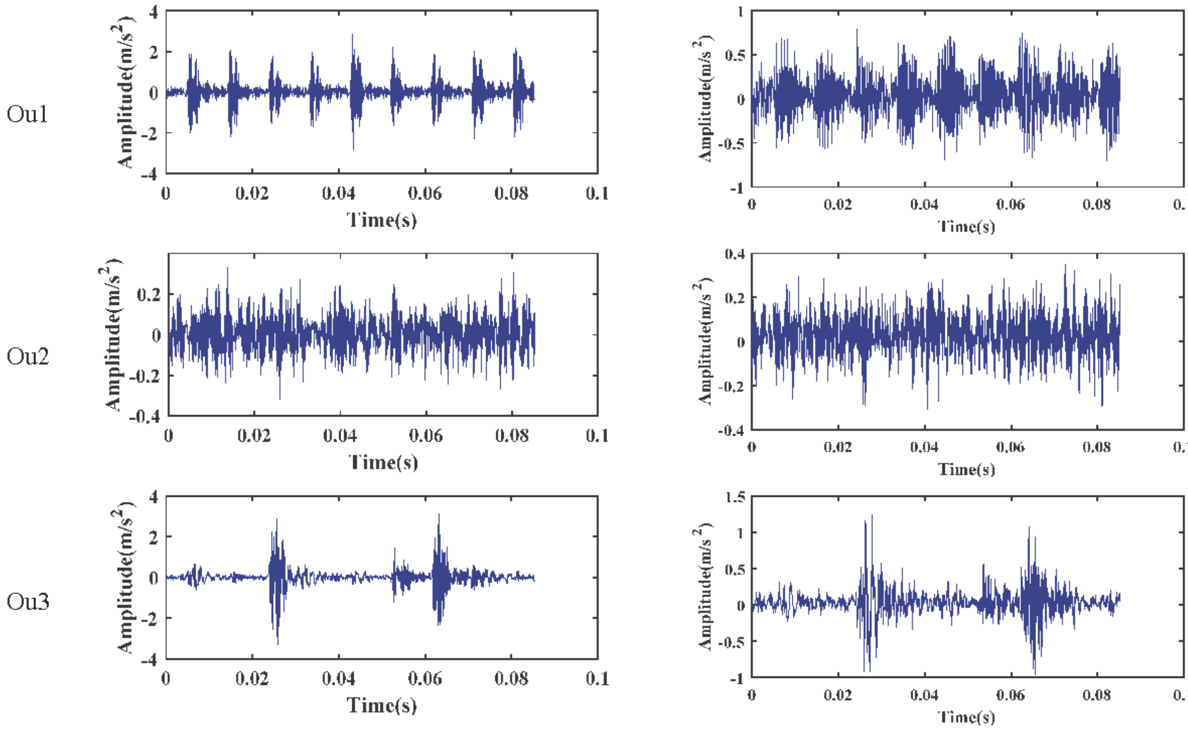

Figure 8 Spectrum of Ba1 vibration signals at the DE and FE (see online version for colours)

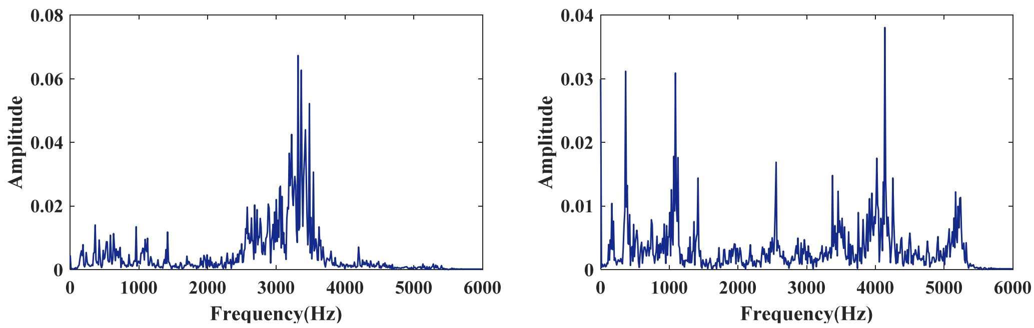

(a) (b)

Table 2 Center frequency of bearing vibration signals of different fault types at DE and FE

Fault type		*Nor*	*Ba1*	*Ba2*	*Ba3*	*In1*	*In2*	*In3*	*Ou1*	*Ou2*	*Ou3*
Initial center	DE	1100	3400	3300	3300	3500	3500	2900	2800	3400	3400
Frequency ω_d/Hz	FE	1000	4100	4100	400	1500	4300	1800	3300	4100	600

Figure 9 Time-domain waveforms before and after the VME algorithm processes the Ba1 vibration signals at the DE and FE (see online version for colours)

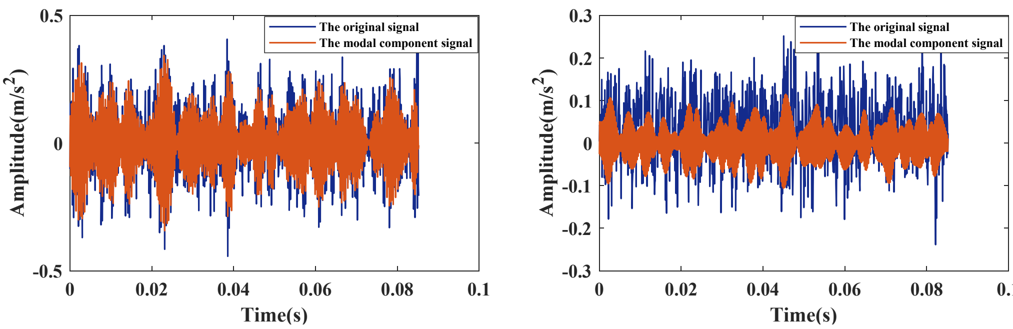

(a) (b)

Figure 10 The spectrum before and after the VME algorithm processes the Ba1 vibration signals at the DE and FE (see online version for colours)

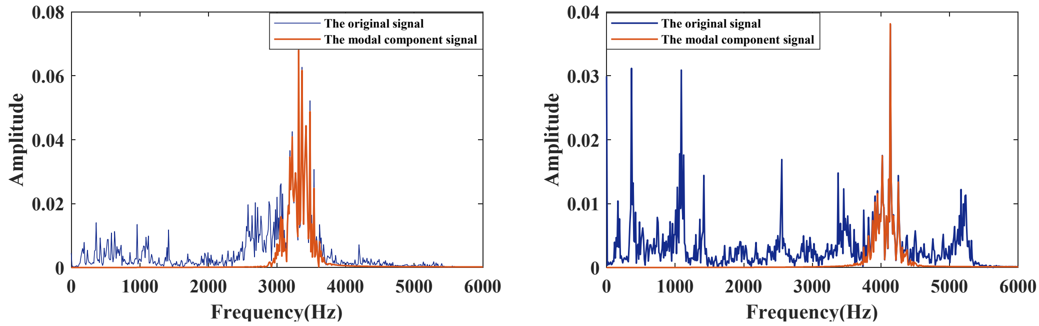

(a) (b)

Figure 11 Greyscale images of different fault types of CWRU

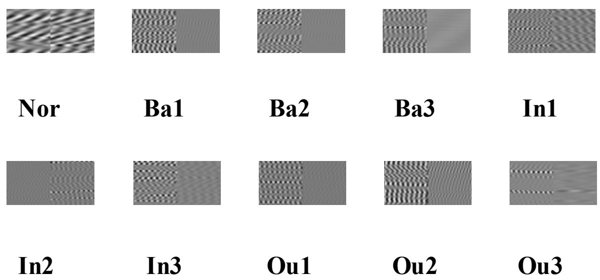

Figure 12 (a) Bypass-SqueezeNet training set and testing set accuracy curve and (b) bypass-SqueezeNet training set and testing set loss function curve (see online version for colours)

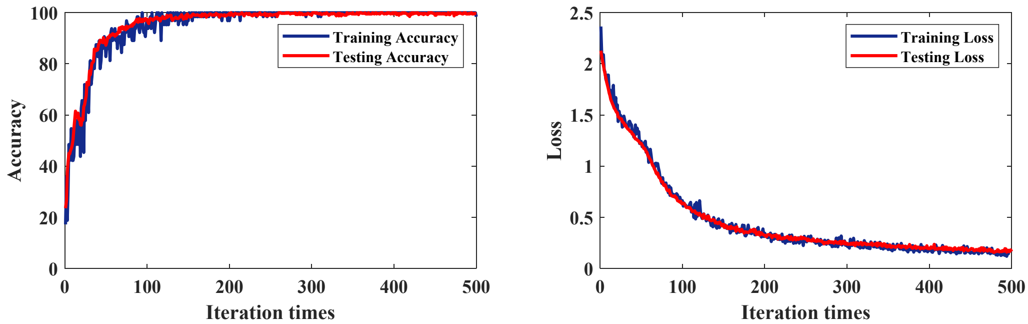

(a) (b)

4.3 Network model parameters

The hyper-parameters of the network model have a very large impact on the training process of the samples as well as the final diagnostic results. In this paper, based on the experience as well as the experimental results, the hyper-parameter settings of the Bypass-SqueezeNet model are determined as shown in Table 3. The loss function curves and accuracy curves of the training and testing of the network model in the whole process are shown in Figure 12, and the pictures show that the model proposed in this paper can achieve 100% accuracy during both training and testing.

4.4 Experimental comparison of different methods

To verify the excellence of the VME in extracting bearing fault features, the VME is compared with four commonly used feature extraction methods: VMD, empirical mode decomposition (EMD), and ITD. The diagnostic results of the above methods are shown in Table 4. Compared to other algorithms, VME spends the least amount of time processing the signal and has the highest rate of diagnostic accuracy when ultimately applied to the model.

Table 3 Hyper-parameters of the bypass-SqueezeNet model

Hyper-parameters	*Parameter setting*
Optimiser	Adam adaptive optimiser
Learning rate	0.001
Batch size	64
Max epoch	20
Loss function	Cross-entropy loss function
Training set	80%
Testing set	20%

Table 4 Diagnosis results and time of different feature extraction methods

Method	*VME*	*VMD*	*EMD*	*ITD*
Accuracy (%)	100	99.75	98	98.75
Time(s)	0.131	2.057	0.182	0.148

At the same time, to demonstrate the effectiveness of using multi-sensor bearing vibration signals for fault diagnosis in this paper, it is compared with the method of using only single-sensor bearing vibration signals for fault diagnosis, and the final results are shown in Table 5. Using signals from multiple sensors for fault diagnosis has a higher accuracy rate, 2.20% higher than DE alone and 3.00% higher than FE alone. It is proven that the proposed method can comprehensively utilise the information obtained from different sensors, avoid the perception limitations and uncertainty of a single sensor, form a more comprehensive recognition of rolling bearings, and improve the accuracy rate of diagnosis.

Table 5 Diagnostic results using different sensor signals

Sensor	*Multisensor*	*DE*	*FE*
Accuracy (%)	100	97.80	97

In the next step, the Bypass-SqueezeNet model is compared with SqueezeNet, AlexNet, SLCNN (Zhong et al., 2022), ShuffleNet-V2 (Zhong et al., 2022), MobileNet-V2 (Zhong et al., 2022), and WT-IResNet (Liang et al., 2022), and in order to have a more comprehensive understanding of the performance of the model, it is analysed in terms of four aspects: accuracy rate, training time, prediction time, and model parameters, and the specific experimental results are shown in Table 6.

Table 6 Performance comparison of different network models

Models	*Bypass-SqueezeNet*	*SqueezeNet*	*AlexNet*	*SLCNN* (*Zhong et al., 2022*)	*ShuffleNet-V2* (*Zhong et al., 2022*)	*MobileNet-V2* (*Zhong et al., 2022*)	*WT-IResNet* (*Liang et al., 2022*)
Accuracy (%)	100	99.2	97.48	99.5	98.2	98.6	100
Training time (s)	83.4	83.8	182.4	–	–	–	661
Prediction time (s)	0.642	0.725	1.867	0.085	0.081	0.120	–
Parameter (MB)	0.049	0.049	143.2	0.95	7.39	5.48	0.132

It can be seen that the Bypass-SqueezeNet model has the highest diagnostic accuracy among all the models, and at the same time, the model has the shortest training time and the fewest model parameters, which is only 0.049 MB, which can greatly reduce the memory usage. Although the model prediction time is not the least, the difference is small compared to other models. Bypass-SqueezeNet has the same number of parameters as SqueezeNet but has much better performance. Meanwhile, compared with the lightweight model SLCNN used in Zhong et al. (2022), the parameter of the Bypass-SqueezeNet model is only 1/19, but it has a higher accuracy rate. In view of various indicators, the Bypass-SqueezeNet model used in this paper shows excellent performance.

4.5 *Diagnostic performance in noisy environment*

The experiments in this section will verify the fault diagnosis performance of the method proposed in this paper in noisy environments by adding Gaussian white noise (WGN) with different signal-to-noise ratios (SNRs) to simulate the complex environments in industrial production. SNR is an indicator used to compare the intensity of the required signal with the intensity of the background noise. The specific formula is as follows:

$$SNR_{db} = 10log_{10}(\frac{P_{signal}}{P_{noise}}) \tag{5}$$

where P_{signal} and P_{noise} are the intensity magnitudes of the signal and noise, respectively.

The GWN with different SNRs is added to the original signals of the two sensors. Due to the space limitation of the paper, taking Ba1 at the DE as an example, Figure 13 shows the time-domain waveform after adding the noise signal. Comparison with the original signal in Figure 7 reveals that the time-domain waveforms are changed after the addition of noise, and the fault characteristics in the original signal are very seriously damaged, which will greatly affect the learning process of the model and lead to a significant reduction in the accuracy of the diagnosis.

In this section, we compare the Bypass-SqueezeNet model with six models, SqueezeNet, AlexNet, ResNet, CNN-LSTM (Hao et al., 2020), IMS-FACNN (Xu et al., 2021b), and VMD-DCNNs (Xu et al., 2020), experimentally, and the experimental results are shown in Table 7. It can be seen that the method used in this paper has the highest accuracy rate in all noise environments. In strong noise environments with SNRs of –4 dB and –2 dB, the accuracy rate of CNN-LSTM, IMS-FACNN, and VMD-DCNNs decreases very significantly, and all of them are lower than 90%. The diagnostic results of the Bypass-SqueezeNet model remain high, with an accuracy rate of around 94%. It is fully proven that the VME algorithm used in this paper can extract the modal components containing the fault characteristics of rolling bearings from the vibration signals with noise. At the same time, the Bypass-SqueezeNet model used in this paper has good learning ability and anti-noise robustness, so as to obtain better performance in a noisy environment.

Figure 13 Time-domain waveform of Ba1 after adding noise at the DE: (a) SNR = –4 dB; (b) SNR = –2 dB; (c) SNR = 0 dB; (d) SNR = 2 dB; (e) SNR = 4 dB and (f) SNR = 6 dB (see online version for colours)

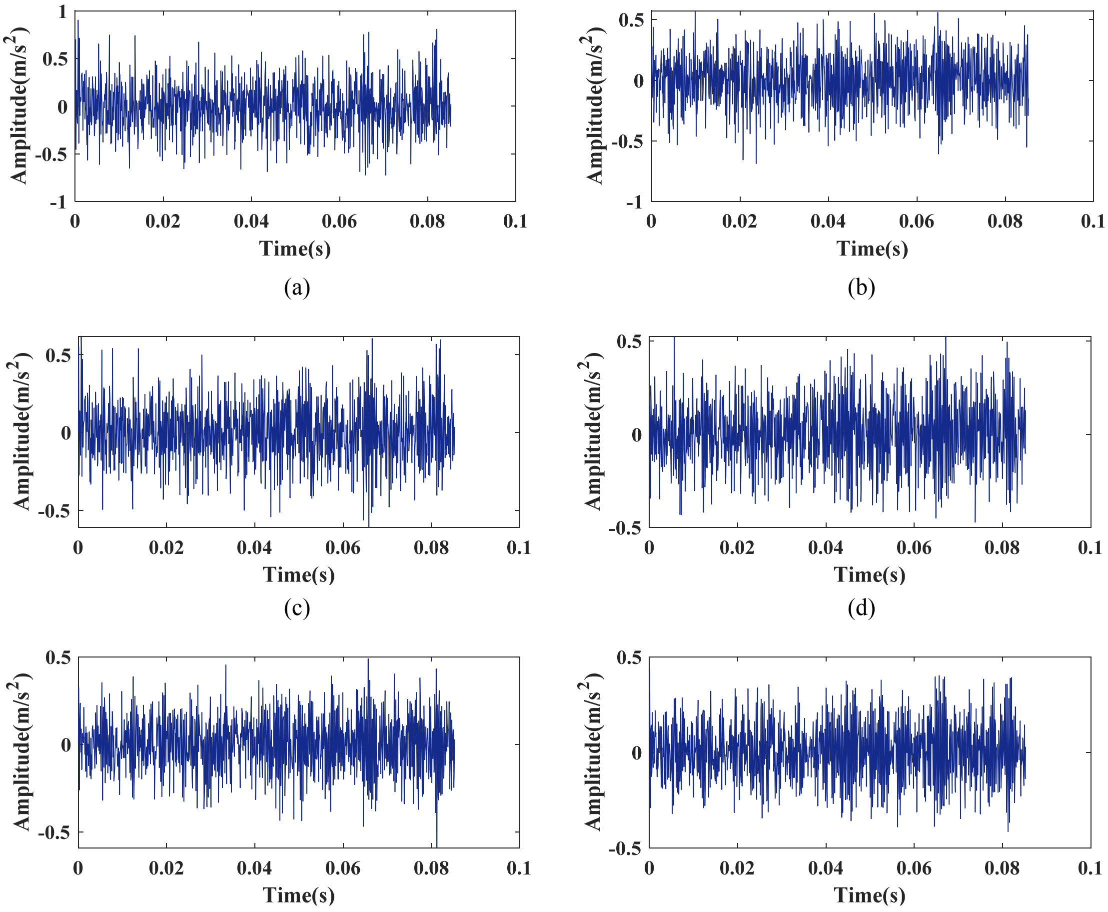

Table 7 Performance comparison of different network models

SNR (dB)	*Models*						
	Bypass-SqueezeNet	*SqueezeNet*	*AlexNet*	*ResNet*	*CNN-LSTM* (*Hao et al., 2020*)	*IMS-FACNN* (*Xu et al., 2021b*)	*VMD-DCNNs* (*Xu et al., 2020*)
–4	93.15	91.80	88.65	86.30	67.00	79.41	64.73
–2	94.45	92.10	90.35	89.85	83.00	83.72	77.00
0	95.85	94.80	93.70	92.05	92.00	92.92	90.42
2	97.00	96.10	93.40	94.30	96.00	96.66	95.00
4	97.55	96.70	96.75	95.10	97.00	97.43	96.59
6	98.95	97.40	97.50	96.15	98.50	98.94	98.59

In order to see the classification effect of the model more intuitively, t-SNE is used to visualise the test samples in different noises, and at the same time, the confusion matrices are created, as shown in Figures 14 and 15, which show that after the training of the Bypass-SqueezeNet model, the output features of the different SNR cases have become very separable, which proves that the network model has a very powerful ability to learn the features. According to the analysis based on the confusion matrices, the models can mostly classify the faulty samples into their own categories with high diagnostic accuracy in different SNR cases, which proves that the method proposed in this paper has excellent fault diagnosis capability in noisy environments.

Figure 14 Feature visualisation in different noise environments: (a) SNR = –4 dB; (b) SNR = –2 dB; (c) SNR = 0 dB; (d) SNR = 2 dB; (e) SNR = 4 dB and (f) SNR = 6 dB (see online version for colours)

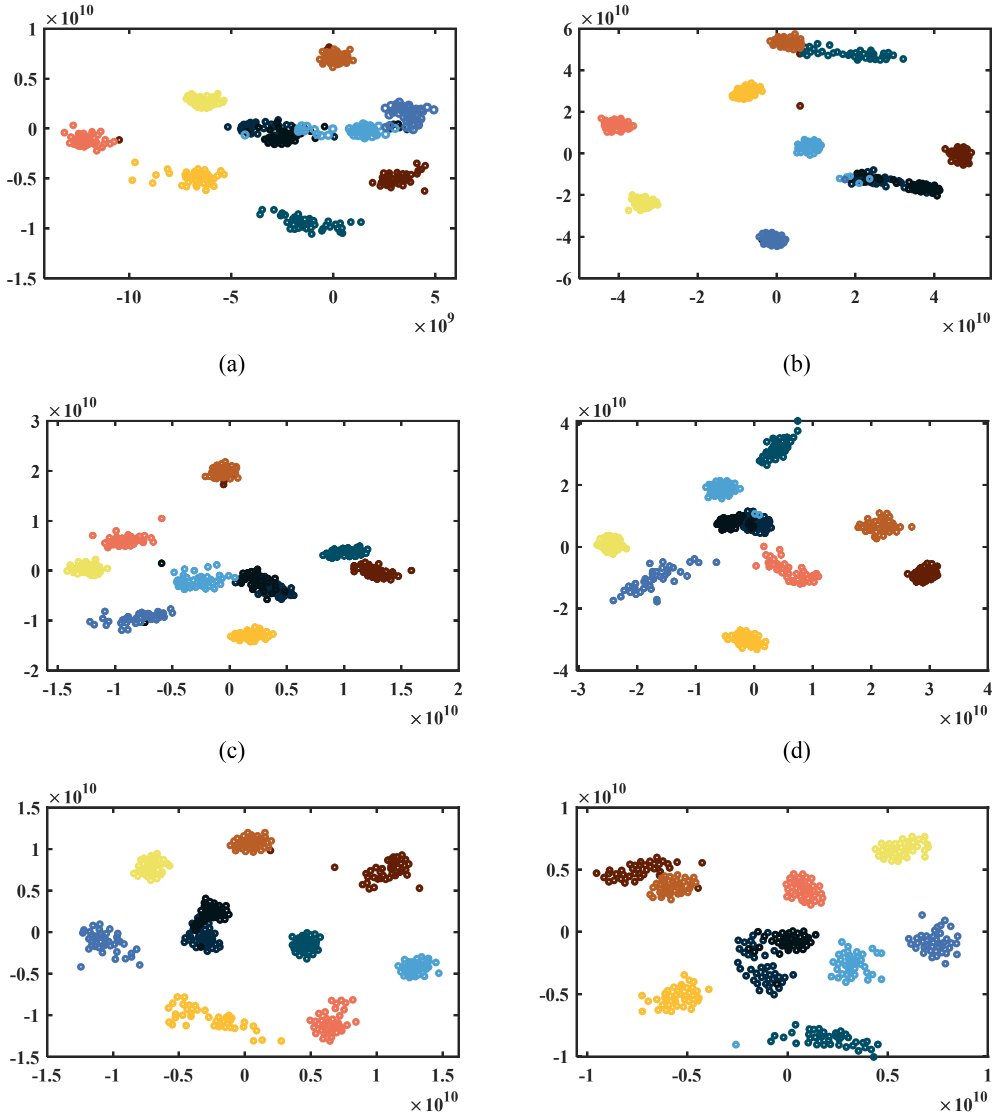

(a) (b) (c) (d) (e) (f)

Figure 15 Confusion matrixes in different noise environments: (a) SNR = –4 dB; (b) SNR = –2 dB; (c) SNR = 0 dB; (d) SNR = 2 dB; (e) SNR = 4 dB and (f) SNR = 6 dB (see online version for colours)

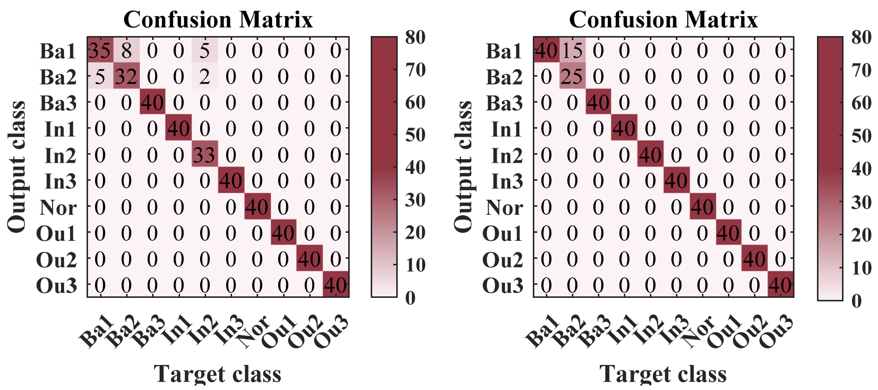

(a) (b)

Figure 15 Confusion matrixes in different noise environments: (a) SNR = –4 dB; (b) SNR = –2 dB; (c) SNR = 0 dB; (d) SNR = 2 dB; (e) SNR = 4 dB and (f) SNR = 6 dB (see online version for colours) (continued)

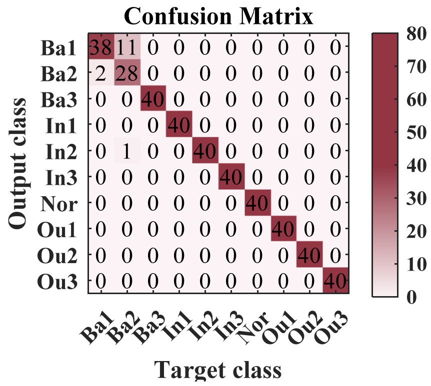

(c)

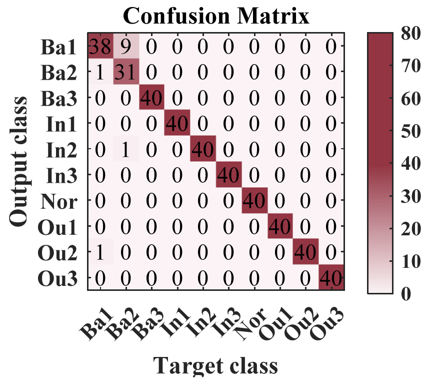

(d)

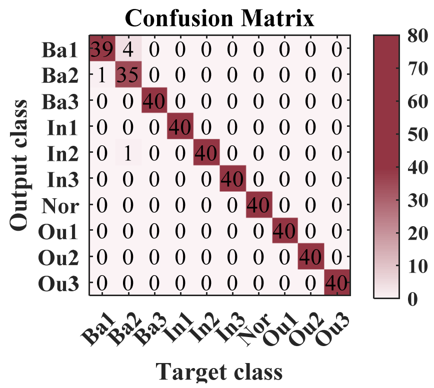

(e)

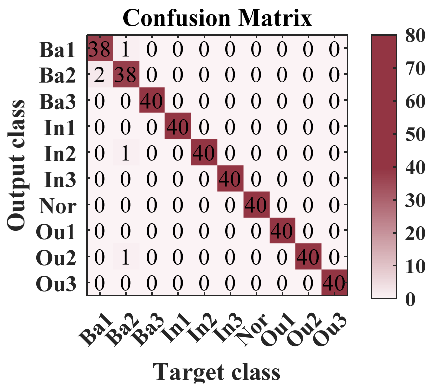

(f)

To test the stability of the Bypass-SqueezeNet model under the influence of noise, experiments are conducted using data with added SNR = –4 dB noise. The samples of 20%, 40%, 60%, and 80% are selected for the training of the model, and the remainder of the samples are used for testing. The final experimental results are shown in Table 8. It can be seen that the Bypass-SqueezeNet model has high diagnostic accuracy in different proportions of sample training situations, and compared with the traditional SqueezeNet model, accuracy has greatly improved, proving that the addition of residual structure helps the model improve its overall performance.

Table 8 Diagnostic accuracy of the model with different proportions of training samples

Training sample proportion (%)	*Accuracy*	
	Bypass-SqueezeNet	*SqueezeNet*
20	88.00%	85.18%
40	91.20%	88.60%
60	92.15%	90.55%
80	93.15%	91.80%

5 Conclusions

In this paper, to address the problems of low accuracy of rolling bearing fault diagnosis in noisy environments as well as the large parameters and slow training speed of deep learning models, we propose a multi-sensor rolling bearing intelligent fault diagnosis method based on VME and a lightweight deep neural network. The method first uses VME to process the vibration signals from different sensors, extracts the desired modal component, constructs grey-scale images based on this component signal, and then uses the lightweight model Bypass-SqueezeNet for training and testing, ultimately obtaining the fault diagnosis results of rolling bearings. Several experiments are conducted on the CWRU dataset, and the final experimental results all show that the method proposed in this paper has high diagnostic accuracy, few model parameters, and excellent overall performance, which fully proves the effectiveness of the method proposed in this paper.

References

Azim Naz, M. and Sarath, R. (2022) 'Optimisation assisted CNN framework for bearing fault diagnosis', *International Journal of Networking and Virtual Organisations*, Vol. 26, pp.291–308.

Feng, Z., Wang, S. and Yu, M. (2023)'A fault diagnosis for rolling bearing based on multilevel denoising method and improved deep residual network', *Digital Signal Processing*, Vol. 140, p.104106.

Hao, S.J., Ge, F.X., Li, Y.M. and Jiang, J.Y. (2020) 'Multisensor bearing fault diagnosis based on one-dimensional convolutional long short-term memory networks', *Measurement*, Vol. 159, p.107802.

Iandola, F.N., Moskewicz, M.W., Ashraf, K., Han, S., Dally, W.J. and Keutzer, K.J.A. (2016) *SqueezeNet: AlexNet-Level Accuracy with 50x Fewer Parameters and < 1MB Model Size*, abs/1602.07360.

Kajkamhaeng, S. and Chantrapornchai, C. (2021) 'SE-SqueezeNet: SqueezeNet extension with squeeze-and-excitation block', *International Journal of Computational Science and Engineering*, Vol. 24, pp.185–199.

Kim, S. (2014) 'Margin-maximised redundancy-minimised SVM-RFE for diagnostic classification of mammograms', *International Journal of Data Mining and Bioinformatics*, Vol. 10, pp.374–390.

Li, C., Liu, Y., Liao, Y. and Wang, J. (2022a) 'A VME method based on the convergent tendency of VMD and its application in multi-fault diagnosis of rolling bearings', *Measurement*, Vol. 198, p.111360.

Li, H., Wu, X., Liu, T., Li, S., Zhang, B., Zhou, G. and Huang, T. (2022b) 'Composite fault diagnosis for rolling bearing based on parameter-optimized VMD', *Measurement*, Vol. 201, p.111637.

Liang, P., Wang, W., Yuan, X., Liu, S., Zhang, L. and Cheng, Y. (2022) 'Intelligent fault diagnosis of rolling bearing based on wavelet transform and improved ResNet under noisy labels and environment', *Engineering Applications of Artificial Intelligence*, Vol. 115, p.105269.

Mourad, T., Lotfi, S., Sabeur, A. and Adnane, C. (2010) 'Recurrent neural network and bionic wavelet transform for speech enhancement', *International Journal of Signal and Imaging Systems Engineering*, Vol. 3, pp.136–144.

Shao, H., Lin, J., Zhang, L., Galar, D. and Kumar, U. (2021) 'A novel approach of multisensory fusion to collaborative fault diagnosis in maintenance', *Information Fusion*, Vol. 74, pp.65–76.

Sheoran, P. and Saini, J.S. (2021) 'Automated blink artefact removal from EEG using variational mode decomposition and singular spectrum analysis', *International Journal of Biomedical Engineering and Technology*, Vol. 36, pp.64–78.

Smith, W.A. and Randall, R.B. (2015) 'Rolling element bearing diagnostics using the case western reserve university data: a benchmark study', *Mechanical Systems and Signal Processing*, Vols. 64-65, pp.100–131.

Walia, E., Singh, C. and Suneja, A. (2015) 'Computationally efficient rotation invariant discrete cosine transform-based semi-blind watermarking technique', *International Journal of Signal and Imaging Systems Engineering*, Vol. 8, pp.286–297.

Wang, S. and Feng, Z. (2024) 'Multi-sensor fusion rolling bearing intelligent fault diagnosis based on VMD and ultra-lightweight GoogLeNet in industrial environments', *Digital Signal Processing*, Vol. 145, p.104306.

Xie, T., Huang, X. and Choi, S.K. (2022) 'Intelligent mechanical fault diagnosis using multisensor fusion and convolution neural network', *IEEE Transactions on Industrial Informatics*, Vol. 18, pp.3213–3223.

Xu, Z.F., Li, C. and Yang, Y. (2020) 'Fault diagnosis of rolling bearing of wind turbines based on the variational mode decomposition and deep convolutional neural networks', *Applied Soft Computing*, Vol. 95, p.106515.

Xu, L., Chatterton, S. and Pennacchi, P. (2021a) 'Rolling element bearing diagnosis based on singular value decomposition and composite squared envelope spectrum', *Mechanical Systems and Signal Processing*, Vol. 148, p.107174.

Xu, Z.F., Li, C. and Yang, Y. (2021b) 'Fault diagnosis of rolling bearings using an improved multi-scale convolutional neural network with feature attention mechanism', *ISA Transactions*, Vol. 110, pp.379–393.

Ye, M., Yan, X., Chen, N. and Jia, M. (2023) 'Intelligent fault diagnosis of rolling bearing using variational mode extraction and improved one-dimensional convolutional neural network', *Applied Acoustics*, Vol. 202, p.109143.

Yu, M. and Pan, X. (2020) 'A novel ITD-GSP-based characteristic extraction method for compound faults of rolling bearing', *Measurement*, Vol. 159, p.107736.

Zhang, D. and Gao, Z. (2013) 'An advanced coevolution scheme for optimisation of artificial neural network', *International Journal of Mechanisms and Robotic Systems*, Vol. 1, pp.316–330.

Zhen, D., Li, D., Feng, G., Zhang, H. and Gu, F. (2022) 'Rolling bearing fault diagnosis based on VMD reconstruction and DCS demodulation', *International Journal of Hydromechatronics*, Vol. 5, pp.205–225.

Zhong, H., Lv, Y., Yuan, R. and Yang, D. (2022) 'Bearing fault diagnosis using transfer learning and self-attention ensemble lightweight convolutional neural network', *Neurocomputing*, Vol. 501, pp.765–777.